Friction **11**(7): 1265–1275 (2023)
https://doi.org/10.1007/s40544-022-0662-1
ISSN 2223-7690
CN 10-1237/TH
RESEARCH ARTICLE

A theoretical justification of the slip index concept in fretting analysis

Ivan I. ARGATOV[1], **Young S. CHAI**[2,*]

[1] *Institut für Mechanik, Technische Universität Berlin, 10623 Berlin, Germany*

[2] *School of Mechanical Engineering, Yeungnam University, Gyeongsan 712-749, Republic of Korea*

Received: 14 October 2021 / Revised: 17 January 2022 / Accepted: 13 June 2022

Abstract: Fretting in the partial-slip and gross-slip regimes under a constant normal load is considered. The tangential force–displacement relations for the forward and backward motions are described based the generalized Cattaneo–Mindlin theory of tangential contact and Masing's hypothesis on modelling the force–displacement hysteretic loop. Besides the critical force and displacement parameters (characterizing the triggering of sliding), the model includes one dimensionless fitting parameter that tunes the tangential contact stiffness of the friction–contact interface. Explicit expressions are derived for the main tribological parameters of the fretting loop, including the slip index and the signal index. The presented phenomenological modelling approach has been applied to the analysis of two sets of experimental data taken from the literature. It has been shown that the experimentally observed simple relation of a rational type between the slip index and the slip ratio corresponds to the gross-slip asymptotics of the corresponding model-based predicted relation. The known quantitative criteria for the transition from the partial slip regime to the gross slip regime are expressed in terms of the stiffness parameter, and a novel geometric transition criterion is formulated.

Keywords: fretting wear; slip index; signal index; partial slip; energy ratio

1 Introduction

The phenomenon of fretting has been observed for a long time [1], and it is still the subject of active tribological research, both experimental [2] and theoretical [3]. Whereas fretting wear, fretting fatigue, and fretting corrosion are frequently encountered in frictional contacts subjected to prolonged tangential oscillations of small amplitude, overall, the accumulated fretting damage may become a critically decisive factor for long-term functionality of the contact interfaces. An important example of serious consequences that may result from fretting wear is associated with flow induced vibrations in the pressurized water reactor system of nuclear power plants [4, 5].

In addition to the stick regime of fretting, which is regarded as a non-dissipating regime [6], there are distinguished two main regimes of fretting wear: partial slip and gross slip, and their distinction from experimentally observed tribological characteristics of a contact interface, such as variations of the tangential force and the relative displacement, is rather to be regarded as one of poorly understood aspects of fretting process [7]. This is mainly because the regime transition occurs when a relative motion is undertaken over the entire contact interface, which is usually hidden from observation in the real engineering applications.

Significant progress in the analysis of the fretting regime transition was achieved when Fouvry et al. [8] introduced certain transition criteria to quantify the boundary between the partial and gross slip. In

* Corresponding author: Young S. CHAI, E-mail: chai868920@gmail.com

particular, based on the classical Cattaneo–Mindlin theory [9, 10] of tangential contact (in a ball on flat contact configuration), the effects of partial slip and dissipated energy were highlighted and, in particular, the so-called slip and energy ratios were suggested as dimensionless transition criteria.

Varenberg et al. [11] have made another important contribution to our understanding of the transition from fretting to reciprocal sliding by introducing a similarity criterion, termed as the slip index, as a result of their dimensional analysis of the mechanics of fretting contact. Further, Varenberg et al. [12] have established a simple empirical relation between the slip ratio and the modified slip index that incorporates the friction coefficient.

In response to the need of monitoring fretting characteristics in real-time, Kim et al. [13] introduced the so-called fretting signal index as a normalized phase difference between the friction force signal and the displacement signal, when one of them vanishes. However, to the best of the authors' knowledge, there are no published reports revealing the interdependence between the different transition criteria introduced so far.

In the present study, we develop a unified mathematical modelling framework, which incorporates as a special case the Cattaneo–Mindlin theory-based models used in Refs. [8, 13]. To keep the analysis simple, we employ a one-free-parameter model for the tangential force loading of a contact–friction interface, which is based on Masing's hypothesis (see, e.g., [14]) for a hysteresis loop formed by the unloading and reloading curves in cyclic loading. In particular, the developed approach allows to theoretically justify the experimentally established relation [12] between the slip index and the slip ratio. As an important result of the presented analysis, we formulate a simple model-free transition criterion, which is based on geometric properties of the slip ratio/slip index variation curve.

2 Theory

2.1 Masing hysteretic model for fretting contact

We consider a contact interface that may experience relative tangential motion under a constant normal load, N. Let F and x denote the tangential force and the corresponding relative displacement, respectively. Moreover, let F_* and x_* denote the critical force and displacement at incipient sliding starting from the position of rest, when the tangential load is gradually increasing. For quasi-static (non-accelerating) sliding, we assume $F = F_*$ and, thus, the tangential force F is balanced by the friction force $F_* = \mu N$, where μ is the Coulomb coefficient of friction.

The functional dependence $F(x)$ of the tangential force F on the tangential displacement x in the case of initial loading is termed as the backbone curve (see Fig. 1). We note that the derivative $\mathrm{d}F(x)/\mathrm{d}x$ is called the incremental tangential stiffness, and its value at the zero point is equal to $\tan(\alpha_0)$, where α_0 is the angle of inclination of a tangent line to the backbone curve at the origin (see Fig. 1). The slop $S_c = \tan(\alpha_0)$ is usually called the (initial) interface contact stiffness. For frictional interfaces, S_c determines the maximum incremental tangential stiffness.

The Masing model for reciprocating quasi-static sliding between the contacting surfaces with the force amplitude F_0 below the critical value, that is $F_0 < F_*$, gives the following analytical expressions for the forward, $\vec{F}(x)$, and backward, $\overleftarrow{F}(x)$, force–displacement curves (see Fig. 2), which are based on a chosen expression $F(x)$ for the backbone curve,

$$\vec{F}(x) = -F_0 + 2F\left(\frac{x_0 + x}{2}\right) \tag{1}$$

$$\overleftarrow{F}(x) = F_0 - 2F\left(\frac{x_0 - x}{2}\right) \tag{2}$$

It is to emphasize that the Masing model exploits the symmetry condition $\overleftarrow{F}(x) = -\vec{F}(-x)$.

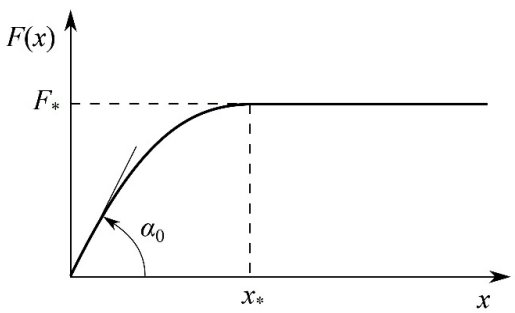

Fig. 1 Backbone curve for the Masing model of the tangential reaction of a fretting contact interface.

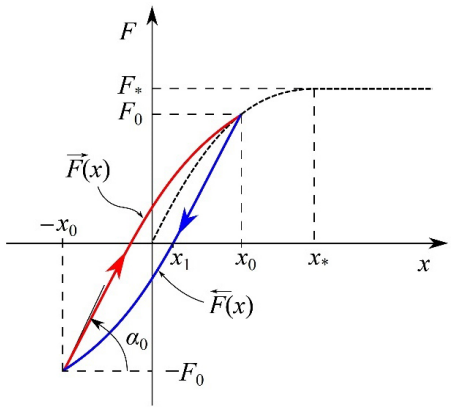

Fig. 2 Schematic diagram for a hysteresis loop of the Masing model in partial slip. (A hysteresis curve, which enters the gross slip stage, has been shown in Fig. 3.)

Following the Ref. [15], we assume that

$$F(x)=\begin{cases}F_*\left[1-\left(1-\dfrac{x}{x_*}\right)^m\right], & 0\le x\le x_*\\ F_*, & x\ge x_*\end{cases} \tag{3}$$

We note that the case $m=3/2$ corresponds to the Cattaneo–Mindlin theory [9, 13] (see also Ref. [8]). In its general form, the Eq. (3) represents the model of tangential reaction of a lap-type joint (we refer to the Ref. [13] for details). In the present study, the exponent parameter $m\ge 1$ is used as a fitting constant, along with the parameters x_* and F_*.

If the displacement amplitude is not large, that is $x_0\le x_*$, then the substitution of Eq. (3) into Eqs. (1) and (2) yields

$$\vec{F}(x)=-F_0+2F_*-2F_*\left(1-\frac{x_0+x}{2x_*}\right)^m \tag{4}$$

$$\overleftarrow{F}(x)=F_0-2F_*+2F_*\left(1-\frac{x_0-x}{2x_*}\right)^m \tag{5}$$

where, in view of Eq. (3), the force and displacement amplitudes are related by

$$\frac{x_0}{x_*}=1-\left(1-\frac{F_0}{F_*}\right)^{1/m} \tag{6}$$

If the displacement amplitude is large, that is $x_0\ge x_*$, then the force amplitude F_0 equals F_*, and thus, Eqs. (1) and (2) imply that

$$\vec{F}(x)=\begin{cases}-F_*+2F\left(\dfrac{x_0+x}{2}\right), & -x_0\le x\le -x_0+2x_*\\ F_*, & -x_0+2x_*\le x\le x_0\end{cases} \tag{7}$$

and

$$\overleftarrow{F}(x)=\begin{cases}-F_*, & -x_0\le x\le x_0-2x_*\\ F_*-2F\left(\dfrac{x_0-x}{2}\right), & x_0-2x_*\le x\le x_0\end{cases} \tag{8}$$

where $F((x_0+x)/2)$ and $F((x_0-x)/2)$ are given by the first line of Eq. (3) upon the substitution of $(x_0+x)/2$ and $(x_0-x)/2$ instead of x, respectively.

The schematic diagram for a hysteresis loop in the case $x_0>x_*$ is shown in Fig. 3. In the case of displacement-controlled loading, when the displacement variable x is specified, the value of the displacement amplitude x_0 may take an arbitrary positive value. In the force-controlled tangential loading, the force amplitude F_0, of course, cannot exceed the critical value F_*.

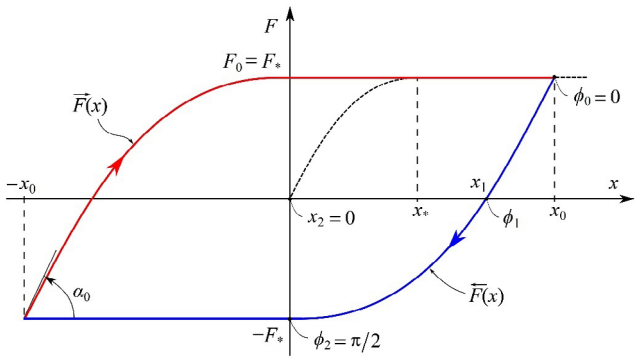

Fig. 3 A characteristic friction loop in the gross slip regime, when $x_0>x_*$.

Remark 1. We recall that Masing's model of hysteresis in symmetric periodic oscillations between the turning points $(-x_0,-F_0)$ and (x_0,F_0) assumes that the forward force–displacement curve $\vec{F}(x)$ can be obtained from the backbone curve $F(x)$ by means of an affine transformation without shearing, that is $\vec{F}(x)=C_1+C_2F(c_1x+c_2)$. The transformation coefficients c_1 and c_2 are defined from the condition that the argument c_1x+c_2 of the function $F(c_1x+c_2)$ should change from 0 to x_0, when the argument x of the function $\vec{F}(x)$ increases from $-x_0$ to x_0. At the same time, the coefficients C_1 and C_2 are determined from the

condition that the corresponding values of $\vec{F}(x)$ should increase from $-F_0$ to F_0. Thus, from the equations $-c_1x_0+c_2=0$ and $c_1x_0+c_2=x_0$, it follows that $c_1=1/2$ and $c_2=x_0/2$, and therefore, by reinforcing the conditions $\vec{F}(-x_0)=-F_0$ and $\vec{F}(x_0)=F_0$, in view of the relation $F_0=F(x_0)$, we readily get $C_1=-F_0$ and $C_2=2$, which is in complete agreement with Eq. (1).

2.2 Slip ratio

We recall [11] that the slip amplitude is defined as the amplitude of the relative displacement between two positions where the tangential force vanishes. In other words, we consider the equations $\vec{F}(x)=0$ and $\bar{F}(x)=0$ and evaluate their solutions $x=-x_1$ and $x=x_1$, respectively. The value of x_1, thus, gives the slip amplitude and by definition satisfies the equation

$$\bar{F}(x_1)=0 \tag{9}$$

The so-called slip (or sliding [8]) ratio is defined as $s=A_s/A_d$, where A_d is the imposed displacement amplitude, and A_s is the resulting slip amplitude. In our notation, where $A_d=x_0$ and $A_s=x_1$, we have

$$s=\frac{x_1}{x_0} \tag{10}$$

When the backbone curve is defined by Eq. (3), it is readily seen that the root of Eq. (9) is independent of F_* (this conclusion also follows from a simple dimensional analysis) and thus depends on the values of the model parameters x_* and m as well as on the value of the imposed displacement amplitude x_0. Hence, the slip ratio will be a function of the dimensionless parameter m and the relative displacement amplitude:

$$\xi=\frac{x_0}{x_*}$$

In view of Eqs. (5) and (8), Eqs. (9) and (10) yield

$$s=\begin{cases}1-\dfrac{2}{\xi}+\dfrac{2-c_m}{\xi}\left(1+(1-\xi)^m\right)^{\frac{1}{m}}, & 0<\xi\le 1\\ 1-\dfrac{c_m}{\xi}, & \xi\ge 1\end{cases} \tag{11}$$

where we have introduced the auxiliary notation $c_m=2-2^{(m-1)/m}$.

It can be verified that Eq. (11) complies with the limit $s\to 0$ as $\xi\to 0$. To this end, the slip ratio is shown to depend only on the imposed relative displacement amplitude $\xi=x_0/x_*$ and the dimensionless stiffness parameter m that tunes the tangential contact stiffness of the friction–contact interface.

2.3 Slip index

We recall that the notion of the slip index, δ, was introduced [11] based on the dimensional analysis of the hysteretic friction loop by the equation $\delta=A_dS_c/N$, where S_c is the tangential stiffness of the contact interface, and N is the normal load. In our notation, we have

$$\delta=\frac{x_0S_c}{N} \tag{12}$$

According to Ref. [11], the stiffness S_c is defined as the slop of the forward force–displacement curve $\vec{F}(x)$ at the beginning of the forward motion (see Fig. 2), that is $S_c=(\mathrm{d}\vec{F}/\mathrm{d}x)\big|_{x=-x_0}$. In view of Eqs. (1) and (7), we easily find that $S_c=(\mathrm{d}F/\mathrm{d}x)\big|_{x=0}$, and therefore, Eq. (3) implies that

$$S_c=m\frac{F_*}{x_*} \tag{13}$$

Thus, the substitution of Eq. (13) into Eq. (12) yields

$$\delta=\mu m\frac{x_0}{x_*} \tag{14}$$

where we have taken into account that $F_*=\mu N$. Thus, in the framework of the developed generalized Cattaneo–Mindlin theory-based model, the slip index is found to be proportional to the coefficient of friction μ, the stiffness parameter m, and the relative displacement amplitude x_0/x_* that we denoted above as ξ.

2.4 Energy ratio

Following Ref. [8], we consider the ratio between the dissipated energy, W_d, and the total energy, W_t, and

denote it by η, that is

$$\eta = \frac{W_{\mathrm{d}}}{W_{\mathrm{t}}} \tag{15}$$

The total energy W_{t} is defined as the energy input, i.e.,

$$W_{\mathrm{t}} = 4x_0F_0 \tag{16}$$

whereas the dissipated energy (per cycle) is given by

$$W_{\mathrm{d}} = \int_{-x_0}^{x_0} \left(\vec{F}(x) - \tilde{F}(x)\right)\mathrm{d}x \tag{17}$$

If the displacement amplitude is not large, that is $x_0 \le x_*$, then the substitution of Eqs. (4) and (5) into Eq. (17) yields

$$W_{\mathrm{d}} = \frac{8mF_*x_*}{m+1}\left\{1-\left(1-\frac{F_0}{F_*}\right)^{1+1/m} - \frac{(m+1)}{2m}\frac{F_0}{F_*}\left(1+\left(1-\frac{F_0}{F_*}\right)^{1/m}\right)\right\} \tag{18}$$

where, in view of Eq. (3), we have

$$F_0 = F_*\left[1-\left(1-\frac{x_0}{x_*}\right)^m\right] \tag{19}$$

Hence, the substitution of Eq. (19) into Eq. (18) leads to the following result

$$W_{\mathrm{d}} = \frac{8mF_*x_*}{m+1}\left\{\left(1-\frac{x_0}{x_*}\right)^{m+1} - 1 + \frac{(m+1)}{2}\frac{x_0}{x_*}\left(1+\left(1-\frac{x_0}{x_*}\right)^m\right)\right\} \tag{20}$$

In particular, when the imposed displacement amplitude coincides with the critical value of displacement, that is $x_0 = x_*$, Eq. (20) yields

$$W_{\mathrm{d}}^* = W_{\mathrm{d}}\big|_{x_0=x_*} = \frac{4(m-1)}{m+1}F_*x_* \tag{21}$$

It is of interest to note that $W_{\mathrm{d}}^* = 0$ in the special case $m = 1$, which corresponds the case of linearly elastic tangential response (without dissipation), when Eq. (3) simplifies as $F(x) = (F_*/x_*)x$ for $0 \le x \le x_*$. It can be simply verified that in the case $m = 1$, Eq. (20) also yields $W_{\mathrm{d}} = 0$ for any $x_0 \in (0, x_*)$.

If the displacement amplitude is large, that is $x_0 \ge x_*$, then the substitution of Eqs. (7) and (8) into Eq. (17) implies that

$$W_{\mathrm{d}} = W_{\mathrm{d}}^* + 4F_*x_*\left(\frac{x_0}{x_*} - 1\right) \tag{22}$$

where W_{d}^* is given by Eq. (21).

Thus, the energy ratio η as a function of the relative displacement amplitude x_0/x_* can be evaluated by Eqs. (15), (16), and (20), when $x_0 \le x_*$, and by Eqs. (15), (22), and (16) with $F_0 = F_*$, when $x_0 \ge x_*$. Observe that the energy ratio simply follows from Eq. (15) by substituting there the expressions given by Eqs. (16) and (20) or (22) followed by simple algebra. However, when the derived formulas are applied for numerical calculations, it is much simpler to program the dissipated ratio $W_{\mathrm{d}}/W_{\mathrm{t}}$ in three simple steps: first, we calculate the total energy W_{t}, second, depending on the value of the relative displacement amplitude, we calculate the dissipated energy W_{d}, using one of Eqs. (20) or (22), and then, we take the ratio of W_{d} to W_{t}.

2.5 Signal index

Regarding the periodic character of fretting oscillations and *per se* following Ref. [13], we introduce the phase of displacement signal ϕ by assuming that

$$x = x_0\cos\phi \tag{23}$$

It is clear (see Fig. 3) that, when the phase angle ϕ (being measured in radians) increases from zero to $\pi/2$, the tangential displacement x decreases from the maximum value x_0 (displacement amplitude) to zero.

Let ϕ_1 denote the phase corresponding to the displacement x_1 defined by Eq. (9). Based on the phase difference between the point $x = x_1$, where the tangential force vanishes, and the point $x = 0$, where the tangential displacement vanishes, we introduce the signal index, χ, as the ratio of the phase difference $\pi/2 - \phi_1$ to the normalizing value $\pi/2$, that is

$$\chi = 1 - \frac{2}{\pi}\phi_1 \tag{24}$$

In view of Eq. (23), the following relations hold true:

$$\phi_1 = \int_0^{\phi_1} \mathrm{d}\phi = -\int_{x_0}^{x_1} \frac{\mathrm{d}x}{\sqrt{x_0^2 - x^2}} = \int_{x_1/x_0}^{1} \frac{\mathrm{d}\theta}{\sqrt{1-\theta^2}}$$
$$= \frac{\pi}{2} - \arcsin\frac{x_1}{x_0}$$

It is pertinent to recall here that, in view of Eq. (23), we have $\phi = \arccos(x/x_0)$ for $x \in [-x_0, x_0]$, and thus, $\mathrm{d}\phi = -(x_0^2 - x^2)^{-1/2}\mathrm{d}x$ for $x \in (-x_0, x_0)$.

Thus, the substitution of the obtained value for ϕ_1 into Eq. (24) yields

$$\chi = \frac{2}{\pi}\arcsin\frac{x_1}{x_0} \tag{25}$$

Observe that though the obtained result simply follows from Eq. (24) and equation $\phi_1 = \arccos(x_1/x_0)$, the calculus-based method allows a straight-forward generalization of Eq. (25) for harmonic oscillations of a general nature.

Finally, we note that, in light of the definition of the slip ratio (see Eq. (10)) Eq. (25) can be represented as $\chi = (2/\pi)\arcsin s$. In other words, in the framework of the developed generalized Cattaneo–Mindlin theory-based model, the signal index χ is uniquely determined by the slip ratio s.

3 Results

3.1 Transition criteria

Following Ref. [8], we consider quantitative characteristics of the transition between a partial and a gross slip behaviour at the fretting contact interface that complies with the Masing hypothesis. According to the assumed backbone curve (3), the transition between the partial slip and gross slip regimes is represented by the condition $x = x_*$. Hence, let s_*, η_*, and χ_* denote the values of s, η, and χ, respectively, evaluated at the transition point $x = x_*$. Then, in view of Eqs. (10), (11), (15), (16), (20)–(22), and (25), we find that

$$s_* = 1 - c_m \tag{26}$$

$$\eta_* = \frac{m-1}{m+1} \tag{27}$$

$$\chi_* = \frac{2}{\pi}\arcsin\left(1 - c_m\right) \tag{28}$$

where $c_m = 2 - 2^{(m-1)/m}$.

We observe that for $m = 1$, all Eqs. (26)–(28) yield zero values, whereas the criteria s_*, η_*, and χ_* are increasing functions of m (see Fig. 4), such that they tend to unit as m tends to infinity.

Figure 5 illustrates a general trend in the variation of the parameters s, η, and χ as functions of the relative displacement amplitude ξ. Without dwelling on details of mathematical analysis, it is of interest to observe that all the considered functions are convex for $\xi < 1$ and concave for $\xi > 1$. In other words, the curvatures of the curves s, η, and χ vs. ξ change their signs when passing the transition point $\xi = 1$.

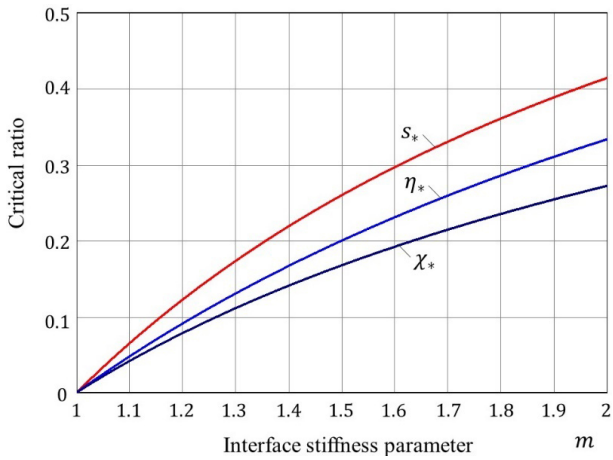

Fig. 4 Transition criteria.

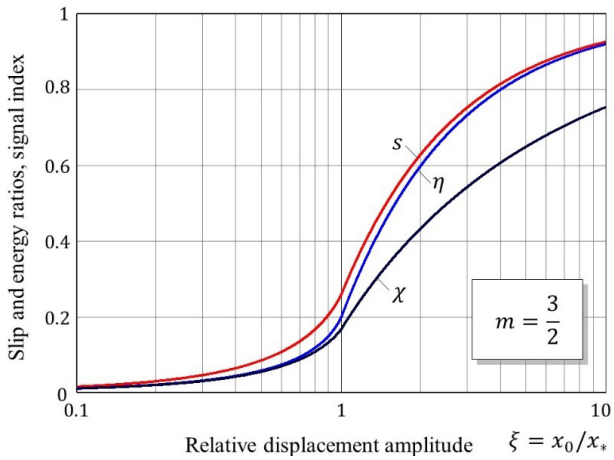

Fig. 5 Variation of the dimensionless parameters s, η, and χ as functions of ξ.

Hence, by generalizing the observed results, we can formulate the following general transition criterion: the transition from partial slip to gross slip is identified with the inflection point of any of the curves s, η, and χ versus the relative displacement amplitude ξ.

3.2 Gross-slip asymptotics

It is of interest to observe that the slip ratio s and the energy ratio η in the gross slip regime are given by simple rational expressions. Indeed, according to Eqs. (11) and (22), we have

$$s = 1 - \frac{c_m}{\xi} \quad \text{for} \quad \xi \geq 1 \tag{29}$$

$$\eta = 1 - \frac{2}{(m+1)}\frac{1}{\xi} \quad \text{for} \quad \xi \geq 1 \tag{30}$$

At the same time, from Eq. (25) we derive the following asymptotic formula:

$$\chi \cong 1 - \frac{2}{\pi}(2c_m)^{\frac{1}{2}}\frac{1}{\sqrt{\xi}}, \quad \xi \gg 1 \tag{31}$$

By comparing Eqs. (31) with (29) and (30), it becomes clear that the signal index slower approaches to the limit value as ξ tends to infinity.

3.3 Variation of the slip ratio vs. the slip index

First, we note that, in view of Eqs. (10) and (14), Eq. (29) can be represented in the form

$$s = 1 - mc_m\frac{\mu}{\delta} \tag{32}$$

where δ is the slip index.

It is of interest to observe that, based on a large number of experimental results, Varenber et al. [12] empirically established the relation $s = 1 - 1.1\mu/\delta$, which is of the form of Eq. (32). By comparing Eqs. (32) with (29), it becomes evident that this experimental law corresponds to the gross-slip asymptotics (see Eq. (29)).

Figure 6 shows the result of fitting of the experimental data for nano- and microscale fretting from Refs. [11, 16], which were represented in Ref. [12] based on average friction coefficient values. It is readily seen that while the simple approximation from Ref. [12] fits well the experimental data in the gross slip regime, the function $s(\delta/\mu m)$, where $s(\xi)$ is given by Eq. (11), is capable of fitting also the data in the partial slip regime.

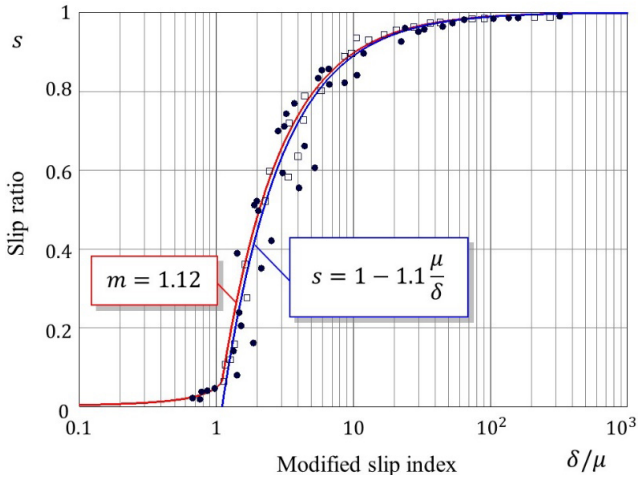

Fig. 6 Variation of the slip ratio s vs. the modified slip index δ/μ. Experimental data is according to Refs. [11, 16].

4 Discussion

As it was already mentioned above, the tangential contact model (see Eqs. (1)–(3)) reduces to the Cattaneo–Mindlin contact model in the special case $m = 3/2$, which corresponds to the Hertzian normal contact. Of course, the adopted phenomenological approach does not provide expressions for F_* and x_* similar to those furnished by the Cattaneo–Mindlin theory of elastic tangential contact. We recall that the latter theory, which assumes the Hertzian contact geometry and isotropy of the material properties, was generalized to arbitrary axisymmetric and non-axisymmetric geometries [17, 18] and transverse isotropy [19]. In particular, if the initial gap between the contacting surfaces, which is measured in the undeformed state in the direction normal to the contact interface, is described by the monomial shape function $\Phi(r) = \Lambda r^{\lambda}$, where r is the polar radius from the centre of circular contact area, then the following relation holds true: $m = (\lambda+1)/\lambda$. Moreover, the case $\lambda = 1$ and, thus, $m = 2$ corresponds to the conical contact geometry, and m decreases to 1 as the shape parameter λ increases to infinity and, thereby, the contacting surfaces become flatter (the limiting case $m = 1$ was noticed in Section 3.1).

The effect of the tangential contact stiffness parameter m on the initial part of the normalized force–displacement relation of the backbone curve is shown in Fig. 7, where the effect of different friction coefficients for partial slip and sliding (static and kinetic coefficients of friction, μ_s and μ_k, according to the terminology [20]) is illustrated as well. The modification of the backbone curve that accounts for different critical values of the tangential force $F_{*s} = \mu_s N$ for $x \le x_*$ and $F_{*k} = \mu_k N$ for $x > x_*$ can be formulated as Eq. (33):

$$F(x) = \begin{cases} F_* \left[1 - \left(1 - \dfrac{x}{x_*} \right)^m \right], & 0 \le x \le x_* \\ \dfrac{\mu_k}{\mu_s} F_*, & x > x_* \end{cases} \tag{33}$$

We underline that, compared to Eq. (3), the above formula introduces only one additional dimensionless parameter, namely, the friction coefficient ratio μ_k / μ_s.

Figure 8 shows the results of fitting the experimental data presented in Ref. [21] by using the model predictions that are based on the backbone curves given by Eqs. (3) and (33) (see curves 1 and 2, respectively). We note that the total energy in the slip regime was evaluated as $W_t = 4x_0 F_*$, where according to Ref. [21], F_* is the maximum tangential force associated with the displacement amplitude x_0. Evidently, the refined model based on Eq. (33) allows a better fit of the energy ratio results, and, in particular,

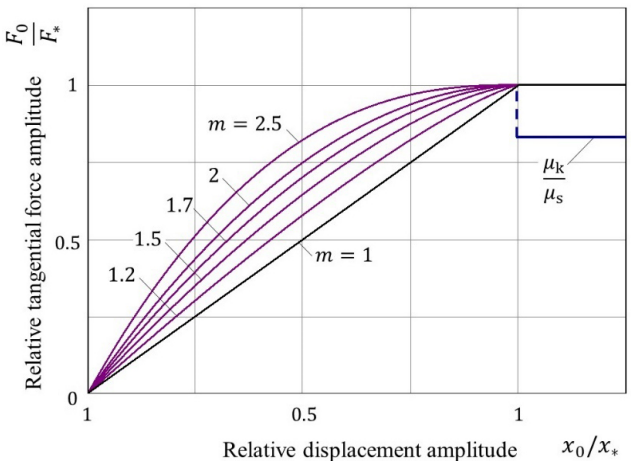

Fig. 7 Effect of the stiffness parameter m on the variation of the backbone curve for $x_0 < x_*$. Effect of the different static and kinetic coefficients of friction ($\mu_s > \mu_k$) on the variation of the backbone curve for $x_0 > x_*$.

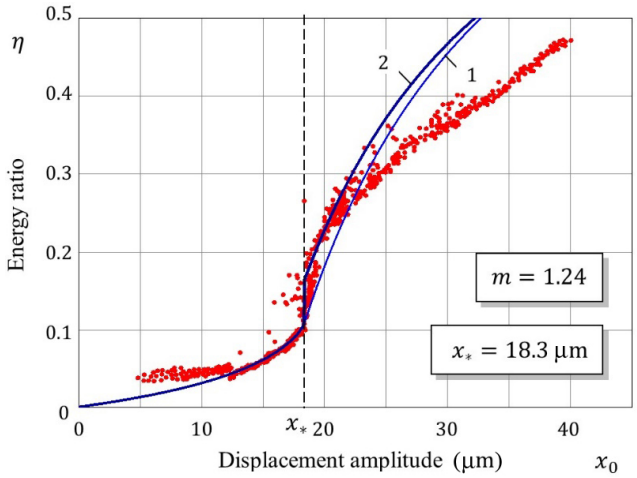

Fig. 8 Variation of the energy ratio η vs. the displacement amplitude x_0. Experimental data is according to Ref. [21]. Curve 1 is drawn based on the constant friction coefficient model; curve 2 takes into account a drop of the friction coefficient from 0.9 to 0.85 in the transition to sliding.

this modified model accommodates the observed jump in the energy ratio upon the transition from partial slip to sliding. It should be emphasized that the ratio μ_k / μ_s was not used as a fitting variable, and its value was evaluated based on the friction coefficients $\mu_s = 0.9$ and $\mu_k = 0.85$ taken from the data presented in Ref. [21].

Yet another point that deserves a comment is a pronounced discrepancy between the model predictions and the experimental data for larger displacement amplitudes (see Fig. 8). Apparently, this can be explained by the effect of the system stiffness, that is of the tangential accommodation of the testing device [8], since the dissipated energy is evaluated as $W_d = W_t - W_e$, where W_e is the elastic energy. That is why, when the elastic energy is also stored in the system besides the contact interface, the share of the dissipated energy W_d in the total energy W_t decreases. At the same time, the models presented above implicitly take into consideration only contact deformations at the contact interface.

Another important result of the presented analysis is that the empirical relation $s = 1 - 1.1\mu/\delta$, which was established in Ref. [12] between the slip ratio s and the slip index δ, represents the so-called gross-slip asymptotics. This, in particular, means that the empirical relation, if applied for determining the transition between the partial and gross slip, may introduce a

systematic error as *a priori* can be expected from any asymptote, provided insufficient experimental data is available for the analysis, and other additional tools of analysis (like the newly introduced convexity/concavity geometric criterion) are not applied.

We recall that differential calculations were applied in Ref. [8] for evaluating the transition point from the maximum of the second derivative of a certain contact parameter (tangential force or dissipated energy) with respect to the contact displacement. It is to note here that the second derivative of the dissipated energy is identically equal to zero in gross slip. However, as Fig. 8 shows, the tribological data is very noisy and, therefore, the application of the numerical differentiation tools is rather problematic. On the contrary, the convexity/concavity transition criterion can be easily implemented, and, moreover, in many cases the transition point may be approximately established by the direct inspection of the plotted data. It should be emphasized that a number of transition criteria have been introduced since the seminal paper by Fouvry et al. [8], but to the best of the authors' knowledge, the simple convexity/concavity transition criterion (without the necessity of specifying the backbone curve) has not been reported in the literature up to now.

It is to note here that the fretting signal index was introduced in Ref. [13] by assuming the harmonic variation of the tangential force, that is like the functional dependence $F = F_0 \cos\varphi$, where φ is the phase angle. However, this approach effectively works only when $F_0 < F_*$, when there is a one-to-one correspondence between the variables F and φ in the base interval $\varphi \in [0,\pi]$. It is also to note here that, though Eq. (23) adopts the first harmonic variation for the tangential displacement x, following the Ref. [13], the dependence of x on the phase angle ϕ can be approximated by the equation $x = x_0 q(\phi)$ with an arbitrary (including saw-like modulation) function $q(\phi)$ which monotonically decreases from its maximum, 1, to its minimum, –1, in the interval $[0,\pi]$. In such a way, Eq. (25) should be replaced by Eq. (24), where ϕ_1 is evaluated as Eq. (34):

$$\phi_1 = \int_0^{\phi_1} \mathrm{d}\phi = -\int_{x_1/x_0}^{1} \frac{\mathrm{d}\theta}{q'(q^{-1}(\theta))} \tag{34}$$

Here, $\phi = q^{-1}(x/x_0)$ is the inverse function for $x/x_0 = q(\phi)$, and $q'(\phi)$ is the derivative of the function $q(\phi)$ with respect to the argument ϕ. To be more precise, Eq. (34) tentatively assumes that the operations of differentiation and integration involved may be defined for the function $q(\phi)$. It is also pertinent to recall here that $q'(q^{-1}(\theta)) = 1/[q^{-1}]'(\theta)$, where $[q^{-1}]'(\theta)$ is the derivative of the function $\phi = q^{-1}(\theta)$. Thus, in view of the assumption that $q^{-1}(1) = 0$, the right-hand side of Eq. (34) can be simplified as $\phi_1 = q^{-1}(x_1/x_0)$.

We observe that Eq. (34) that adopts the change of the phase angle ϕ from zero (maximum displacement) to π (minimum displacement) is convenient for theoretical analysis. In real-time monitoring, the displacement signal comes as a discrete function of time. As such, we may assume that $x = f(t)$, where $f(t)$ is a periodic function of the time variable t varying between $-x_0$ (minimum) and x_0 (maximum) with a period T, so that $f(t+T) = f(t)$. Let t_0, t_1, and t_2 be time moments corresponding respectively to the subsequent points x_0, x_1, and $x_2 = 0$ (see Fig. 3). The phase angle can be introduced in the usual way as $\phi = \omega t + \phi_0$, where $\omega = 2\pi/T$ is the angular frequency of oscillations. Thus, we can write

$$\chi = \frac{2}{\pi}\int_{\phi_1}^{\phi_2} \mathrm{d}\phi = \frac{2\omega}{\pi}\int_{t_1}^{t_2} \mathrm{d}t = -\frac{4}{T}\int_0^{x_1} \frac{\mathrm{d}x}{f'\left(f^{-1}(x)\right)} \tag{35}$$

We note that in practise, one needs only the middle equation in relation Eq. (35), which simply reduces to $\chi = (4/T)(t_2 - t_1)$.

As it has been already mentioned at the end of Section 2.5, the signal index χ is simply related to the slip ratio s, and to the best of the author's knowledge, this fact was not highlighted before. We recall that the signal index, as it was introduced by Kim et al. [13], has shown to be effective for monitoring fretting characteristics in real-time, and therefore, a novel point of view on this transition index developed in the present study (where we have brought under a single mathematical modelling umbrella different transition indexes and criteria known in fretting analysis) is, without any doubts, of practical importance for tribologists.

It is to note here that the notions of the "static" and "kinetic" coefficients of friction have been introduced above following to Blau [20]. It is clear that from a

so-called microscopic point of view, the transition from rest to gross slip involves microslips between asperities forming the rough surfaces. However, the related questions about the variation of the coefficient of friction at the contact interface lie outside of the scope of the present study, as they refer to the micro-scale modelling approach. On the contrary, in the present study we necessarily take a so-called macro-scale point of view, as the slip index is measured from the macro-scale characteristics of fretting loops.

Finally, we observe that the presented above simple mathematical modelling framework can be further generalized to account for the effect of variation of the backbone curve due to wear. Recently, the phenomenon of non-monotonic behaviour of the dissipated energy in the partial-slip regime of fretting wear was highlighted in Refs. [22, 23]. In this way, the stiffness parameter m (which is shown to be dependent on the contact geometry) is likely to become dependent on the number of fretting cycles due to the contact geometry adaptation. Another possible generalization concerns the application of artificial neural networks (ANNs) (see, e.g., Ref. [24]) for the purpose of realistic description of the backbone curve based on experimentally observed data for the tangential force–displacement relation in the fretting loop.

5 Conclusions

In the present study, a unified mathematical modelling approach for the analysis of the tangential force–displacement hysteretic loops in fretting has been developed based on Masing's hypothesis about the scaling of the forward and backward force–displacement curves from the backbone curve. By adopting a one-free-parameter generalized Cattaneo–Mindlin contact model of the frictional tangential contact loading, explicit relations for the main tribological parameters of the fretting loop (slip and energy ratios among others) have been derived. As a result, novel transition criterions, which are parameterized by the interface stiffness parameter, have been introduced, including the convexity/concavity geometric criterion that is shown to be a model-free transition criterion.

Acknowledgements

This work was supported by the 2021 Yeungnam University Research Grant.

References

[1] Tomlinson G A. The rusting of steel surfaces in contact. *Proc Roy Soc London. Ser. A* **115**(771): 472–483 (1927)

[2] Meng Y G, Xu J, Jin Z M, Prakash B, Hu Y Z. A review of recent advances in tribology. *Friction* **8**(2): 221–300 (2020)

[3] Zhang Z N, Pan S H, Yin N, Shen B, Song J. Multiscale analysis of friction behavior at fretting interfaces. *Friction* **9**(1): 119–131 (2020)

[4] Lee C Y, Bae J W, Chai Y S, Shin K. Experimental study on impact fretting wear of Inconel tubes under high temperature and pressure. *Int J Modern Phys B* **25**(31): 4253–4256 (2011)

[5] Cai Z B, Li Z Y, Yin M G, Zhu M H, Zhou Z R. A review of fretting study on nuclear power equipment. *Tribol Int* **144**: 106095 (2020)

[6] Vingsbo O, Söderberg S. On fretting maps. *Wear* **126**(2): 131–147 (1988)

[7] Lavella M. Partial-gross slip fretting transition of martensitic stainless steels. *Tribol Int* **146**: 106163 (2020)

[8] Fouvry S, Kapsa P, Vincent L. Analysis of sliding behaviour for fretting loadings: Determination of transition criteria. *Wear* **185**(1–2): 35–46 (1995)

[9] Cattaneo C. Sul contatto di due corpi elastici: Distribuzione locale degli sforzi. *Rend Accad Naz* **27**: 342–348 (1938)

[10] Mindlin R D. Compliance of elastic bodies in contact. *J Appl Mech* **16**: 259–268 (1949)
[11] Varenberg M, Etsion I, Halperin G. Slip index: A new unified approach to fretting. *Tribol Lett* **17**(3): 569–573 (2004)
[12] Varenberg M, Etsion I, Altus E. Theoretical substantiation of the slip index approach to fretting. *Tribol Lett* **19**(4): 263–264 (2005)
[13] Kim J S, Cho D H, Lee K M, Lee Y Z. The signal parameter for monitoring fretting characteristics in real-time. *Tribol Trans* **55**(6): 730–737 (2012)
[14] Segalman D J, Starr M J. Inversion of Masing models via continuous Iwan systems. *Int J Non-Linear Mech* **43**(1): 74–80 (2008)
[15] Argatov I I, Butcher E A. On the Iwan models for lap-type bolted joints. *Int J Non-Linear Mech* **46**(2): 347–356 (2011)
[16] Varenberg M, Etsion I, Halperin G. Nanoscale fretting wear study by scanning probe microscopy. *Tribol Lett* **18**(4): 493–498 (2005)
[17] Jäger J. Axi-symmetric bodies of equal material in contact under torsion or shift. *Arch Appl Mech* **65**: 478–487 (1995)
[18] Ciavarella M. Tangential loading of general three-dimensional contacts. *ASME J Appl Mech* **65**: 998–1003 (1998)
[19] Chai Y S, Argatov I I. Local tangential contact of elastically similar, transversely isotropic elastic bodies. *Meccanica* **53**(11): 3137–3143 (2018)
[20] Blau P J. The significance and use of the friction coefficient. *Tribol Int* **34**(9): 585–591 (2001)
[21] Heredia S, Fouvry S. Introduction of a new sliding regime criterion to quantify partial, mixed and gross slip fretting regimes: Correlation with wear and cracking processes. *Wear* **269**(7–8): 515–524 (2010)
[22] Chai Y S, Argatov I I. Fretting wear accumulation in partial-slip circular Hertzian contact. *Mech Res Comm* **96**: 45–48 (2019)
[23] Argatov I I, Bae J W, Chai Y S. A simple model for the wear accumulation in partial slip Hertzian contact. *Int J Appl Mech* **12**(7): 2050074 (2020)
[24] Argatov I. Artificial Neural Networks (ANNs) as a novel modeling technique in tribology. *Front Mech Eng* **5**: 30 (2019)

Ivan I. ARGATOV. He graduated from Leningrad State University in 1991 where he got diploma in mechanics, and, in 1995, received C.Sc. (equiv. to Ph.D.) degree in solid mechanics. In 2000, he obtained D.Sc. degree (Habilitation) from Saint Petersburg State University. He is a recipient of several awards including the Leonard Euler Fellowship (Deutsche Mathematiker Vereinigung, 1994), Mikhail Lomonosov Fellowship (DAAD, 2004), the Ikerbasque Fellowship for senior researchers (The Basque Foundation for Science, 2010), the Marie Curie Fellowship for experienced researchers (European Commission, 2010), and the Ba-Yu Scholar (Chongqing City, 2020). He is author and co-author of more than a hundred publications in international journals, three monographs, and two graduate textbooks. Currently he is a visiting professor at College of Aerospace Engineering, Chongqing University, China.

Young S. CHAI. He graduated from Seoul National University in 1979 where he got bachelor degree in nuclear engineering, and, in 1981, received M.S. in mechanical engineering from Korea Advanced Institute of Science and Technology (KAIST), Republic of Korea. In 1990, he obtained Ph.D. degree from University of Texas at Austin in engineering mechanics. He has been a professor at School of Mechanical Engineering in Yeungnam University, Republic of Korea, since 1981. His research interests include friction and wear, stress analysis, and interfacial fracture mechanics. Currently he is a professor of emeritus at Yeungnam University, Republic of Korea.